



Production and characterization of femtosecond laser-written double line waveguides in heavy metal oxide glasses



Diego Silvério da Silva^a, Niklaus Ursus Wetter^{a,*}, Wagner de Rossi^a,
Luciana Reyes Pires Kassab^b, Ricardo Elgul Samad^a

^a Centro de Lasers e Aplicações, Instituto de Pesquisas Energéticas e Nucleares – IPEN-CNEN/SP, 2242 A. Prof. Lineu Prestes, São Paulo, Brazil

^b Laboratório de Tecnologia em Materiais Fotônicos e Optoeletrônicos, Faculdade de Tecnologia de São Paulo, CEETEPS, 01124-060, São Paulo, Brazil

ARTICLE INFO

Article history:

Received 31 August 2017
Received in revised form
5 October 2017
Accepted 21 October 2017
Available online 6 November 2017

Keywords:

Femtosecond laser
Double line waveguide
Heavy metal oxide glass
Passive optical component

ABSTRACT

We report the fabrication and characterization of double line waveguides directly written in tellurite and germanate glasses using a femtosecond laser delivering 30 μJ , 80 fs pulses at 4 kHz repetition rate. The double line waveguides produced presented internal losses inferior to 2.0 dB/cm. The output mode profile and the M^2 measurements indicate multimodal guiding behavior. A better beam quality for the $\text{GeO}_2 - \text{PbO}$ waveguide was observed when compared with $\text{TeO}_2 - \text{ZnO}$ glass. Raman spectroscopy of the waveguides showed structural modification of the glassy network and indicates that a negative refractive index modification occurs at the focus of the laser beam, therefore allowing for light guiding in between two closely spaced laser written lines. The refractive index change at 632 nm is around 10^{-4} , and the structural changes in the laser focal region of the writing, evaluated by Raman spectroscopy, corroborated our findings that these materials are potential candidates for optical waveguides and passive components. To the best of our knowledge, the two double line configuration demonstrated in the present work was not reported before for germanate or tellurite glasses.

© 2017 Elsevier B.V. All rights reserved.

1. Introduction

A considerable research effort in the area of femtosecond (fs) laser pulses used to locally modify the structure and refractive properties of optical glasses and other dielectrics via nonlinear absorption, has been conducted in recent years [1]. Because the pulse length of this type of laser is shorter than the electron phonon interaction, one can obtain a process without thermal effects and produce tiny structures, such as waveguides, in transparent materials [2]. Depending on the material properties, as well as on the characteristics of the laser used for inscribing, two types of waveguides can be obtained: the first type consists of a single line, where the modification of the material causes a refractive index increase, leading to light confinement [3]. The second type consists of stress-induced positive refractive index changes in the region adjacent to the writing [4], or negative refractive index changes in the laser focal region [5]. In the latter case, the light is guided in between two or more written lines. The methodology used in this work is based

on the second type of writing, where double line waveguides demonstrated good results, after previous experiments testing both types of writing. Double line waveguides have been demonstrated in a number of hosts, including crystals [4,6–10]. Single line waveguides have the advantage of simpler and faster processing and have also been demonstrated in a variety of glasses including fused silica, borosilicate [11], chalcogenides [12] and BK7 [13]. Double line waveguides are an alternative technique for materials whose properties do not permit the confinement and propagation of light by a single written line and, in principle, permit guiding in an almost unperturbed and pristine region of the bulk material once laser writing occurs at the border of the guiding region.

The fs laser writing methodology has proven to be reliable and is able to compete with clean room processing in terms of waveguide loss, with the advantage that laser writing enables fast prototyping and requires much lower cost of ownership and complexity of fabrication.

Heavy metal oxide glasses, like germanates and tellurites, are interesting materials for photonic applications due to properties such as their high linear refractive index (~ 2) that is responsible for a high nonlinear refractive index, their extensive transmission window from visible to near infrared and lower cutoff phonon

* Corresponding author.

E-mail address: nuwetter@ipen.br (N.U. Wetter).

energy ($<700 \text{ cm}^{-1}$) when compared to silicate, borate, and phosphate glasses. Previously we reported on the fabrication and characterization of active waveguides in $\text{GeO}_2\text{-PbO-Ga}_3\text{O}_3$ glass samples doped with Er^{3+} , written by a femtosecond laser delivering pulses of 80 fs duration at 1 kHz repetition rate. Single line waveguides were formed under different laser pulse energies and scan velocities and the passive and active optical properties of the waveguides were investigated [14].

This work presents, to the best of our knowledge, the first demonstration of waveguiding by the double-line technology using the fs laser writing process in germanate and tellurite glasses.

2. Experimental

2.1. Preparation of glasses

Conventional melting and quenching method was used for the preparation of the glasses. High purity starting oxide powders (99.999%) were melted in platinum ($\text{TeO}_2\text{-ZnO}$) or aluminum ($\text{GeO}_2\text{-PbO}$) crucibles, then poured into heated brass molds (pre-heated at annealing temperature), annealed to reduce the internal stress and then cooled to room temperature inside the furnace. The temperature and time duration for melting and annealing are presented in Table 1, for each glass composition.

2.2. Waveguide writing

The femtosecond laser setup consists of a Ti:Sapphire laser system operating at $\lambda = 800 \text{ nm}$, able to deliver up to 800 μJ of energy in a pulse with duration ranging from 25 to 200 fs, in a 4 kHz repetition rate pulse train (Femtopower Compact Pro HR/HP, from Femtolasers). Sample translation stages with 300 nm precision were controlled via an integrated CadCam system. The parameters used for writing the waveguides are shown in Table 2. Several pairs of closely spaced, parallel waveguides were written using a 20X objective lens with $\text{N.A.} = 0.4$, focal length = 10 mm and depth of focus = 200 μm , separated by a distance of 10 μm , using laser energies of 3 μJ and 30 μJ . The waveguides were written 0.7 mm beneath the sample's surface. After waveguide writing, the glasses were re-polished at the input and output facets that were damaged during the femtosecond writing process. The final length of the obtained waveguides was 1.0 cm.

2.3. Materials and waveguide characterization

The absorbance of the samples was measured with a spectrometer (Cary 5000) to analyze the composition of the samples at the laser focus. For this measurement, a sample with a large number of closely spaced waveguides was prepared. Optical transmission microscopy was used to capture the images of the laser written structures. Fig. 1 shows the setup used to determine the near field profile (using a CCD camera), optical losses (using a Powermeter) and beam quality factor M^2 (using a measurement system formed by a CMOS controlled by a LabVIEW™ program) of a coupled HeNe beam. The optical losses were determined using equation (1), where P_2 represents the output power measured for a

Table 2
Parameters used in the writing process.

Writing speed (mm/min)	1.0
Laser spot size (μm)	5.0
Pulse duration (fs)	80
Wavelength (nm)	800
Polarization to writing direction	parallel
Repetition rate (kHz)	4
Depth of focus (μm)	200

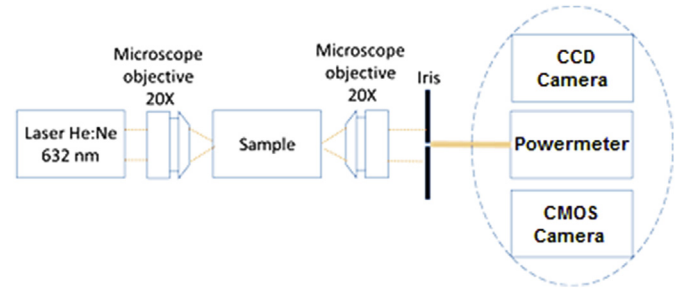


Fig. 1. Basic schematic diagram used to determine the near field profile, optical losses and M^2 factor.

sample of length Z_2 , and P_1 the output power of a sample with reduced length Z_1 [15],

$$\text{Optical losses} = -\frac{10 \log\left(\frac{P_2}{P_1}\right)}{Z_2 - Z_1} \quad (1)$$

To estimate the refractive index change of the waveguides, the output diameter at $1/e^2$ width was measured at a distance of several centimeters, and the numerical aperture (N.A.) of the waveguides was calculated from the ratio between the distance and the mode radius. The refractive index change can be estimated by the measured N.A. of the waveguide, as described in Ref. [15] by the basic equation $\text{N.A.} = \sqrt{n_1^2 - n_2^2} \approx \sqrt{2n_2\Delta n}$, where n_1 and n_2 represent the refractive index of the core and the cladding, respectively. Raman spectroscopic measurements were made in the focal region of the writing and in the bulk glass using a confocal Raman Microscope (WITEC, model: Alpha300) at $\lambda = 532 \text{ nm}$, power of 45 mW, wavenumber within the range of 0–3793 cm^{-1} , 50X objective and resolution of 0.464 μm .

3. Results and discussions

Fig. 2 shows the absorption spectra of $\text{TeO}_2\text{-ZnO}$ and $\text{GeO}_2\text{-PbO}$ glasses taken from the bulk and also from the waveguides written by 30 μJ pulses. Comparing both results we observe a change in the transmittance window mainly for $\text{GeO}_2\text{-PbO}$ glasses. These defects may be attributed to nonlinear absorption of the fs laser beam that generates defects such as oxygen deficient centers and non-bridging oxygen hole centers [16,17].

Fig. 3a shows an image of the waveguide's exit facet,

Table 1
Parameters of the fabrication of the bulk glasses.

Glass	Composition (wt%)	Melting/annealing temperature ($^\circ\text{C}$)	Melting/annealing time (min)
$\text{TeO}_2\text{-ZnO}$	TeO_2 : 18.0	800/325	20/120
	ZnO : 72.0		
$\text{GeO}_2\text{-PbO}$	GeO_2 : 40.3	1200/420	60/60
	PbO : 59.7		

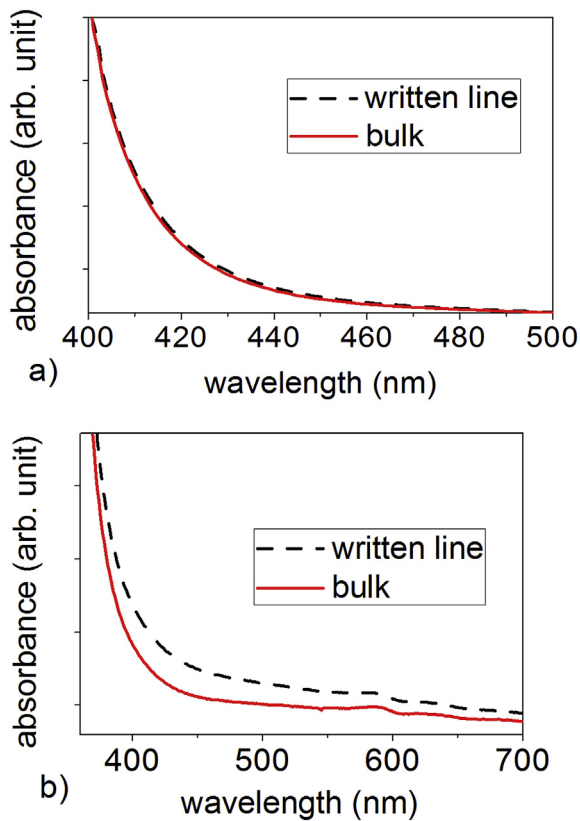


Fig. 2. Absorption spectra of the samples (bulk and fs written area) a) $\text{TeO}_2 - \text{ZnO}$, b) $\text{GeO}_2 - \text{PbO}$.

demonstrating the damage caused at the surface by the fs laser, requiring re-polishing of the facet after laser processing. The arrows indicate the exact location where guiding is observed, which is right in the middle between the loci of the foci from the laser. Fig. 3b shows a double line waveguide composed of two writings separated from each other by $10 \mu\text{m}$, using a pulse energy of $30 \mu\text{J}$. Each dark line in Fig. 3b corresponds to the border of a $6 \mu\text{m}$ wide region affected by the writing process. Guiding occurs in between the two centerlines.

To determine the optical losses using equation (1), two samples with length $Z_2 = 1.0 \text{ cm}$ and a reduced length $Z_1 = 0.6 \text{ cm}$ were prepared. The results are shown in Table 3 where we notice that the lowest optical losses are obtained in both glasses for a pulse energy of $30 \mu\text{J}$.

The near field profiles at the output of the waveguides are shown in Fig. 4. Comparing the results of $\text{TeO}_2 - \text{ZnO}$ and $\text{GeO}_2 - \text{PbO}$ glasses we observe that the near field profiles are different. Fig. 4b and c shows the double line waveguide modes for the lowest loss waveguides ($\text{GeO}_2 - \text{PbO}$ and $\text{TeO}_2 - \text{ZnO}$ written with $30 \mu\text{J}$).

The refractive index change was determined for the waveguides with the lowest optical losses, fabricated with $30 \mu\text{J}$ pulses. The estimated refractive index changes at 632 nm were $\Delta n = 1 \cdot 10^{-4}$ and $\Delta n = 8 \cdot 10^{-4}$ for the $\text{TeO}_2 - \text{ZnO}$ and $\text{GeO}_2 - \text{PbO}$ glasses, respectively.

The M^2 measurements were performed using a standard procedure [18]. The widths and heights of the distributions were calculated at the $1/e^2$ -level to obtain beam propagation factors along perpendicular axes (horizontal x and vertical y) as are shown in Fig. 4. We obtained $M_x^2 = 7.24$ and $M_y^2 = 6.82$ for the $\text{GeO}_2 - \text{PbO}$ waveguide and of $M_x^2 = 4.62$ and $M_y^2 = 6.04$ for the $\text{TeO}_2 - \text{ZnO}$ waveguide.

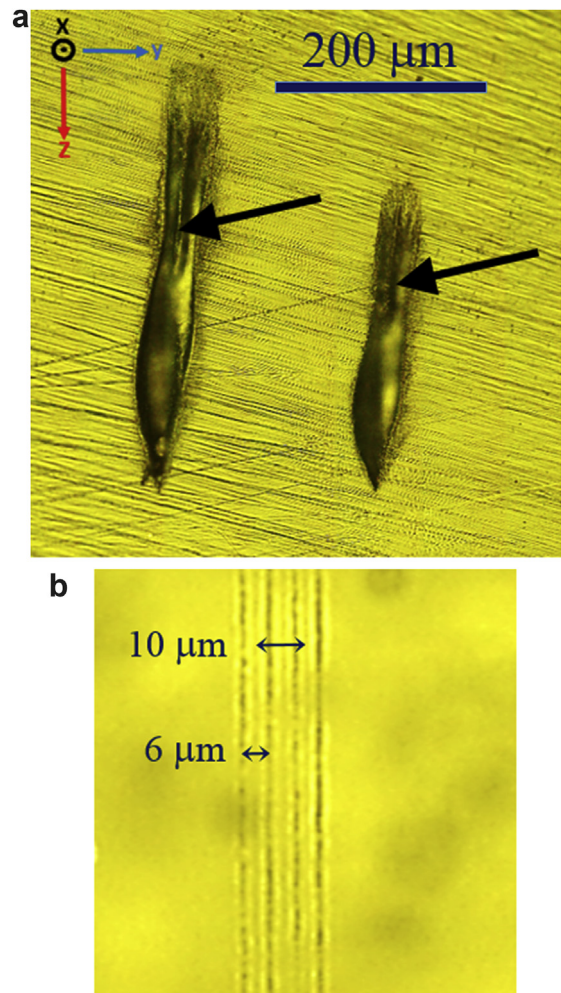


Fig. 3. (a) Close-up photo of the output facet of the $\text{TeO}_2 - \text{ZnO}$ sample showing the effect of the fs laser writing at $30 \mu\text{J}$ (left) and $3 \mu\text{J}$ laser (right) pulse energy. Black arrows indicate the region of waveguiding. The direction of the laser beam is along the z axis and the direction of waveguiding is along the x axis. (b) Top view microscope image of two written double line waveguides in the $\text{GeO}_2 - \text{PbO}$ fabricated with $30 \mu\text{J}$ laser pulse energy.

Table 3
Optical loss results for the sample written with different laser energies.

Glass	Optical loss (dB/cm) $30 \mu\text{J}$	Optical loss (dB/cm) $3 \mu\text{J}$
$\text{TeO}_2 - \text{ZnO}$	1.25	9.95
$\text{GeO}_2 - \text{PbO}$	1.75	6.25

Results from Raman spectroscopic measurements of the laser focal region in the waveguides are shown in Figs. 5 and 6 for the $\text{TeO}_2 - \text{ZnO}$ and $\text{GeO}_2 - \text{PbO}$ glasses, respectively. The Raman spectra were deconvoluted into different Gaussian peaks and the corresponding results are described in Tables 4 and 5. It is important to note that results generated from Raman measurements in the region between the double lines are similar to the bulk glass, which suggests that no structural change is caused by the fs laser writing technique at the locus of wave guiding. Comparing Fig. 5a and b we observe that the boson peak around 200 cm^{-1} in the $\text{TeO}_2 - \text{ZnO}$ spectra, which is related to low frequency-vibrations and characteristic of amorphous materials, is higher with respect to all other peaks in the fs laser written region (solid curve).

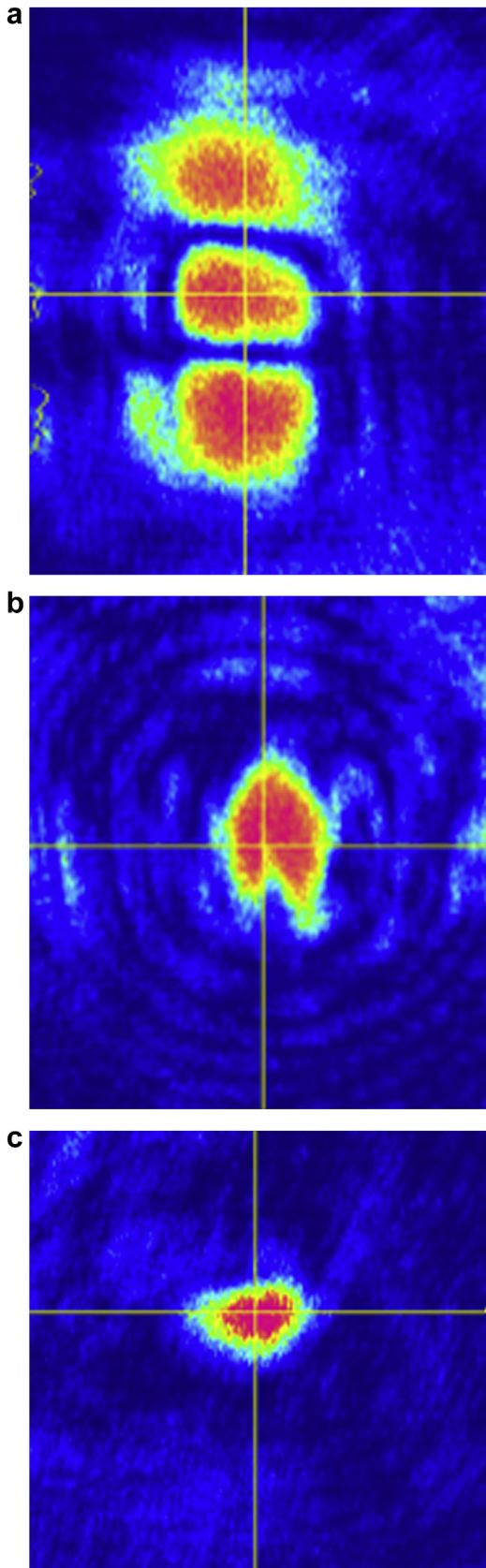


Fig. 4. Near field mode profile (at 632 nm) of the beams transmitted by the waveguides: (a) and (b) GeO₂ – PbO waveguides written with 3 μJ and 30 μJ laser energy, respectively. (c) TeO₂ – ZnO waveguides written with 30 μJ pulse energy.

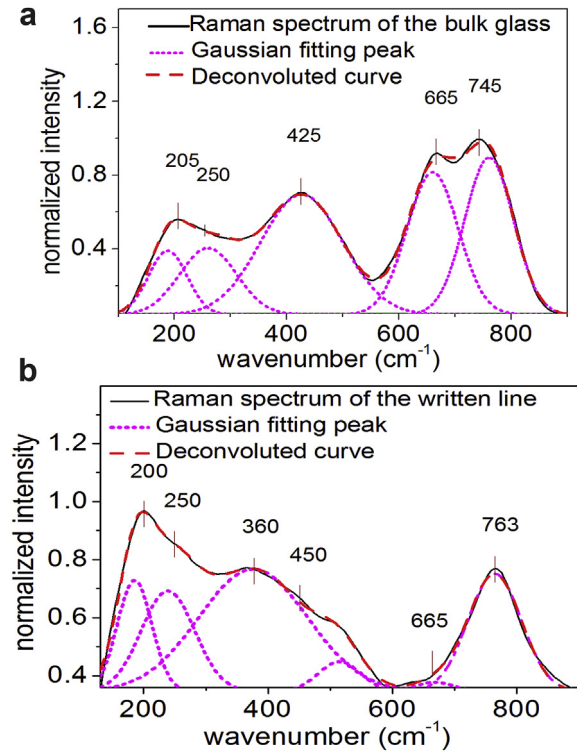


Fig. 5. Deconvoluted Raman Spectra of TeO₂–ZnO glass: (a) Bulk area, (b) written area.

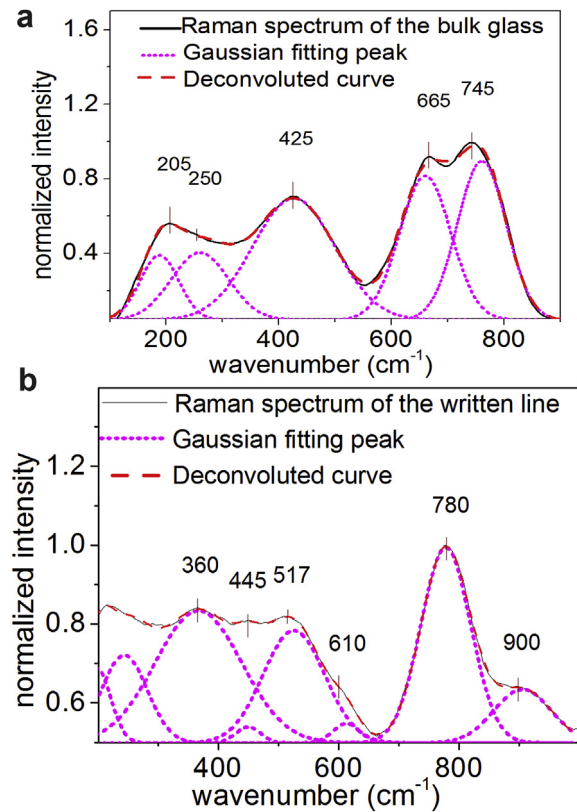


Fig. 6. Deconvoluted Raman Spectra of GeO₂–PbO glass: (a) Bulk area, (b) written area.

Normally the amplitude of the boson peak decreases as a function of increasing structural order of the sample [19]. This indicates a

Table 4
Raman peak positions and assignment of TeO₂ – ZnO glass system.

Peak position (cm ⁻¹)	Assignment
200	Boson area: low-frequency vibrational feature characteristic of amorphous materials [20].
254	ZnO ₄ Bending vibrations of Zn-O bonds in ZnO ₄ tetrahedrons [21].
360	Oscillations of Te-O bonds in TeO ₄ tetrahedra characteristic of α-TeO ₂ [22].
423	Bending vibrations of Zn-O and Te-O-Te linkages formed by corner sharing of (TeO ₄), (TeO ₃₊₁) polyhedra and TeO ₃ units [22].
665	Antisymmetrical TeO ₄ vibration [22–25].
745–763	Vibration of Te-O of TeO ₃ /TeO ₃₊₁ [26].

Table 5
Raman peak positions and assignment of GeO₂ – PbO glass system.

Peak position (cm ⁻¹)	Assignment
200	Boson area: low-frequency vibrational feature characteristic of amorphous materials [20].
330–360	Ge-O-Ge bending modes vibrations [27].
420&445	Symmetric stretching vibrations of Ge-O-Ge bonds [27].
509	Symmetric stretching vibrations along the Ge-O-Ge chain [27].
610	Vibrations of Ge-O bonds in GeO ₆ octahedral units [27].
780	Ge-O- and GeO-Ge symmetric stretching vibrations in GeO ₄ tetrahedral units [27].
900	Asymmetric stretching vibrations of Ge-O-Ge bonds [27].

less connected structural matrix or the formation of basic units different from the bulk glass.

The peak at 250 cm⁻¹, related to ZnO₄ bending vibrations of Zn-O bonds in ZnO₄ tetrahedrons [20] is also higher than the other peaks (except the aforementioned 200 cm⁻¹ peak) in the fs written area (solid line, Fig. 5b). As this was not observed in bulk glass we come to the conclusion that the fs laser written affects the ZnO bonding vibrations of the glass modifier.

The 360 cm⁻¹ peak related to Te-O bonds of α-TeO₂ [21] appears only on the written region. This indicates a change of the size relation between basic units of the network in the fs-written region, since the 360 cm⁻¹ peak is related to a stable crystalline phase, created by the laser writing process, that practically does not exist in the bulk glass.

The peak around 425 cm⁻¹ (seen in bulk glass) is related to bending vibrations of Zn-O and Te-O-Te linkages formed by corner sharing of (TeO₄), (TeO₃₊₁) polyhedrons and TeO₃ units. This peak quenches and shifts to 450 cm⁻¹ for the written region, which suggests that the laser writing causes breaking of the bonds of Te-O-Te and Te-O-Zn [22].

The peak around 665 cm⁻¹, which is strong in the bulk glass, practically does not exist in the written region (Fig. 5(b)). This peak is related to antisymmetrical TeO₄ vibrations and generally assumes large amplitudes in tellurite glasses [22–25]. The results indicate that the antisymmetrical TeO₄ vibration almost does not exist in the written region, and represents another structural change caused by the laser writing process.

Finally, the shift from 745 cm⁻¹ (bulk) to 763 cm⁻¹ (written region) suggests a lesser ordination of pyramidal TeO₃ units, which is a trigonal basic unit of tellurite glasses formed by broken bonds of Te-O [26].

Comparing GeO₂-PbO bulk and waveguides, a more similar behavior of the Raman results can be observed (Fig. 6). The shift of 509 cm⁻¹ (bulk) to 517 cm⁻¹ (written region), related to symmetric stretching vibrations along the Ge-O-Ge chain [27], indicates smaller density of these type of bonds in the written region. The other peaks at 610, 780 and 900 cm⁻¹ are related, respectively, to vibrations of Ge-O bonds in GeO₆ octahedral units, Ge-O- and GeO-Ge symmetric stretching vibrations in GeO₄ tetrahedral units and asymmetric stretching vibrations of Ge-O-Ge bonds [27]. These peaks are similar for both cases (bulk and fs-written region) indicating no influence of the laser writing process.

N. Parveen et al. [28] showed that in samples with a glassy

network formed by a mixture of TeO₄/TeO₃₊₁ and GeO₄ structural units, the increase of TeO₃₊₁/TeO₃ units leads to a decrease of refractive index. The observed decrease of TeO₄ in the written region of our samples suggests that these units have been transformed into TeO₃ causing a negative refractive index modification. The unchanged region between both lines has a positive relative index when compared to adjacent written region and therefore is capable of guiding the light. In the case of the GeO₂ – PbO, the only observed evidences of structural modification caused by the writing process is the Raman shift of 509 cm⁻¹ (bulk) to 517 cm⁻¹ (written region) and the change of the transmittance window (see Fig. 3b).

The laser irradiation is a complex event and thermomechanical effects can occur due to the laser exposure. Raman data showed that thermal accumulation by exposure to femtosecond laser pulses results in areas of overall expansion of the glassy network, demonstrated by a decrease in refractive index [9]. These changes depend on the femtosecond laser writing conditions specifically when the modification is dominated by heat accumulation. Generally, the phenomena of waveguiding between written lines or tracks is attributed to damage [7] of the material inside the track, followed by stress that induces positive refractive index change in the adjacent regions [4,6]. The results of negative refractive index change shown in this work contrasts with other works about laser written channel waveguides in other similar glasses, specially heavy metal oxide glasses [5,12,23,29] where the written single line or track is the waveguide itself.

Table 6 shows information about the writing process in different glasses. In Ref. [5] the formation of the waveguide was attributed mainly to the decrease in La and P atomic concentrations at the center of the channel and a migration of these atoms towards the periphery of the channels, resulting in a modulation of Te:P ratio across the irradiated region. This modulation enabled a positive refractive index change across each channel. In Ref. [12] a mechanical characterization, the nanoindentation, is correlated with variations in the Raman response of exposed glass, which are found to be in good agreement with each other, confirming the structural change caused by the writing process. These results showed two distinct regions due to photo induced modifications. For phosphor-tellurite glasses it was also demonstrated that the migration of tellurium caused a positive index change zone whereas the sodium migration to the tellurium deficient zone allowed the formation of a relatively low index change zone [29]. Two waveguides were

Table 6
Parameters of writing processes in other relevant works.

Glass composition	TeO ₂ , P ₂ O ₅ , Al ₂ O ₃ , La ₂ O ₃ , Er ₂ O ₃ [5]	GeGaS – Er ₂ O ₃ [12]	TeO ₂ , Na ₃ P ₃ O ₉ , ZnO, ZnF ₂ , Er ₂ O ₃ , CeO ₂ , Yb ₂ O ₃ [23,29]	Photo thermal refractive glass (PTR) [8]	N-SF8 glass [10]
Writing laser configuration	Ti: Sapphire laser	Master oscillator power amplified Yb – doped fiber laser	Yb:KYW femtosecond laser	Ti: Sapphire regenerative amplifier ultrafast laser	Amplified Yb:KGW system
Writing speed (mm/min)	0.1 to 0.3	4 to 18	2 to 6	12	120 to 3000
Objective Lens/N.A	25X/0.45	aspheric/0.67	60X aspheric	20X/0.42	100X plan achromat/1.25
Pulse duration (fs)	45	350	400	160	230
Wavelength (nm)	806	1047	1040	800	515
Polarization to writing direction	–	circular	perpendicular	perpendicular	perpendicular
Repetition rate (kHz)	1	100	1000	50	500
Energy (μJ)	3	0.1 to 1.81	0.03	1	0.1 to 0.8

discussed using different writing speeds (2 and 4 mm/s) and it was observed that, depending on the writing speed, tellurium migration was responsible for material densification that permitted the creation of waveguides.

Table 6 also presents the writing parameters used for silicate glasses, reported very recently [8,10], that also used the double line configuration. In the case of the Scott-NSF8 glass [10] it was possible to confine the optical mode by writing two lines separated by 14 μm. The decrease of the refractive index was associated to an increase of the glass volume attributed to glass network modifications.

In both waveguides studied in the present work, the structural modifications induced by laser irradiation probably caused a volume change that enabled the decrease of the refractive index as was observed for the above mentioned Scott-NSF8 glass. To the best of our knowledge, the two double line configuration demonstrated in the present work was not reported before for germanate or tellurite glasses and the present results contribute for a better understanding of the writing process in heavy metal oxide glasses. We recall that no guiding was observed in our samples with a single line, although we tested a large range of laser parameters.

4. Conclusions

This work has addressed the feasibility of producing passive waveguides in heavy metal oxide glasses by direct fs laser writing. The writing parameters were optimized using different energies, scan speeds, polarizations and depth of focus. The best results were obtained for the results described in Table 2.

Raman results showed a much stronger structural change for the TeO₂ – ZnO waveguide when compared to GeO₂ – PbO. The latter showed similar Raman results in the bulk and in the fs written region. When comparing the Raman results in the bulk and in between the double lines of fs-written waveguides, no difference in Raman results were observed, showing no modification of the glassy network in the region between the lines where the guiding occurs.

The photo-induced refractive index change is $-1 \cdot 10^{-4}$ and $-8 \cdot 10^{-4}$ for the TeO₂ – ZnO and GeO₂ – PbO glasses, respectively. Better beam quality was obtained for 30 μJ pulse energy in both glasses, when compared to 3 μJ, with the best M² value measured for the GeO₂ – PbO glass waveguide. The M² values indicate a x,y-symmetrical, multimodal guiding of good quality for both glasses.

The results obtained in the present work are promising for the fabrication of passive components based on germanate and

tellurite glasses, once the guiding area remains unaltered by the fs laser. Further optimization can be expected from improvements in the writing setup such as higher precision of the linear translation stages and a wider range of parameters such as energy, frequency, pulse duration, etc.

Acknowledgment

We acknowledge financial support from Fundação de Amparo à Pesquisa do Estado de São Paulo (FAPESP) (2016/02326-9 and 2013/26113-6).

References

- [1] M. Ams, G.D. Marshall, P. Dekker, J.A. Piper, M.J. Withford, Ultrafast laser written active devices, *Laser Phot. Rev.* 3 (2009) 535.
- [2] R.E. Samad, L.M. Machado, N.D. Vieira Jr, W. d. Rossi, Ultrashort laser pulses machining, in: I. Peshko (Ed.), *Laser Pulses – Theory, Technology, and Applications*, vol. 143, InTech, 2012.
- [3] D. Homoelle, S. Wielandy, Alexander L. Gaeta, Infrared photosensitivity in silica glasses exposed to femtosecond laser pulses, *Opt. Lett.* 24 (18) (1999) 1311.
- [4] N. Pavel, G. Salamu, F. Voicu, F. Jipa, M. Zamfirescu, T. Dascalu, Efficient laser emission in diode-pumped Nd:YAG buried waveguides realized by direct femtosecond-laser writing, *Laser Phys. Lett.* 10 (2013), 095802.
- [5] P. Nandi, G. Jose, C. Jayakrishnan, S. Debbarma, K. Chalapathi, K. Alti, A.K. harmadhikari, D. Mathur, Femtosecond laser written channel waveguides in tellurite glass, *Opt. Lett.* 14 (25) (2006) 12145.
- [6] J. Siebenmorgen, T. Calmano, K. Petermann, G. Huber, Highly efficient Yb:YAG channel waveguide laser written with a femtosecond-laser, *Opt. Exp.* 18 (2010).
- [7] Q. Bin, L. Yang, D. Guo-Ping, L. Fang-Fang, S. Liang-Bi, S. Sheng-Zhi, Q. Jian-Rong, Femtosecond laser-written waveguides in a bismuth germanate single crystal, *Chin. Phys. Lett.* 26 (7) (2009) 070601.
- [8] Y.J. Zhang, et al., Double line and tubular depressed cladding waveguides written by femtosecond laser irradiation in PTR glass, *Opt. Mater. Express* 7 (2017) 2626.
- [9] L.B. Fletcher, et al., Changes to the network structure of Er-Yb doped phosphate glass induced by femtosecond laser pulses, *J. Appl. Phys.* 106 (2009).
- [10] B. Sotillo, et al., Raman spectroscopy of femtosecond laser written low propagation loss optical waveguides in Schott N-SF8 glass, *Opt. Mat.* 72 (2017) 626.
- [11] Huan Huang, Lih Mei Yang, Jian Liu, Femtosecond fiber laser direct writing of optical waveguide in glasses, in: *Proceedings Volume 8164, Nanophotonics and Macrophotonics for Space Environments V*, 81640B, Event: SPIE Optical Engineering + Applications, 2011, San Diego, California, USA, 2011.
- [12] A. Ayiriveetil, T. Sabapathy, G.S. Varma, U. Ramamurthy, S. Asokan, Structural and mechanical characterization on ultrafast laser written chalcogenide glass waveguides, *Opt. Mater. EXPRESS* 6 (N°8) (2016).
- [13] C. Florea, K.A. Winick, Fabrication and characterization of photonic devices directly written in glass using femtosecond laser pulses, *J. Light. Technol.* 21 (2003) 1.
- [14] D.M. da Silva, L.R.P. Kassab, M. Olivero, T.B.N. Lemos, D.V. da Silva, A.S.L. Gomes, Er³⁺ doped waveguide amplifiers written with femtosecond laser in germanate glasses, *Opt. Mater* 33 (2011) 1902.
- [15] Ajoy Ghatak, K. Thyagarajan, *An Introduction to Fiber Optics*, Cambridge

- University Press, 1998.
- [16] T. Asai, Y. Shimotsuma, T. Kurita, A. Murata, S. Kubota, M. Sakakura, K. Miura, F. Brisset, B. Poumellec, M. Lancry, Systematic control of structural changes in GeO₂ glass induced by femtosecond laser direct writing, *J. Am. Ceram. Soc.* 98 (5) (2015) 1471.
- [17] N. Manikandan, Aleksandr Rysasnyanskiy, Jean Toulouse, Thermal and optical properties of TeO₂ – ZnO – BaO glasses, *J. Non. Cryst. Solids* 358 (2012) 947.
- [18] D. Feise, G. Blume, H. Dittrich, Chr. Kaspari, K. Paschke, G. Erbert, High-brightness 635 nm tapered diode lasers with optimized index guiding, *Proc. SPIE* 7583 (2010), 75830V-1-75830V-12.
- [19] V.K. Malinovsky, A.P. Sokolo, The nature of boson peak in raman scattering in glasses, *Solid State Commun. Solid-State Commun.* 57 (9) (1986) 757.
- [20] F. He, Z. He, J. Xiel, Y. Li, IR and raman spectra properties of Bi₂O₃-ZnO-B₂O₃-BaO quaternary glass system, *Am. J. Anal. Chem.* 5 (2014) 1142.
- [21] I.V.G. Amaya, M.E. Zayas, J.A. Rivera, E. Álvarez, S.A.G. Heredia, G.A. Limón, R.L. Morales, J.M. Rincón, Spectroscopic studies of the behavior of Eu³⁺ on the luminescence of cadmium tellurite glasses, *Hindawi Publ. Corp. J. Spectrosc.* 478329 (2015).
- [22] V. Sreenivasulu, G. Upender, V. Chandra Mouli, M. Prasad, Structural, thermal and optical properties of TeO₂-ZnO-CdO-BaO glasses doped with VO²⁺, *Spectrochim. Acta A Mol. Biomol. Spectrosc.* 148 (2015) 215.
- [23] T.T. Fernandez, S.M. Eaton, G.D. Valle, R.M. Vazquez, M. Irannejad, G. Jose, A. Jha, G. Cerullo, R. Osellame, P. Laporta, Femtosecond laser written optical waveguide amplifier in phospho-tellurite glass", *Opt. Express* 18 (19) (2010) 20291.
- [24] A. Chagraoui, I. Yakine, A. Tairi, A. Moussaoui, M. Talbi, M. Naji, Glasses formation, characterization, and cristal-structure determination in the Bi₂O₃-Sb₂O₃-TeO₂ system prepared in an air, *J. Mater. Sci.* 46 (2011) 5439.
- [25] A.K. Yadav, P. Singh, A review of structure of oxide glasses by Raman spectroscopy, *RSC Adv.* 5 (2015) 67583.
- [26] Santos, Fábio Alencar dos, "Geração de segundo harmônico em vidros teluritos TeO₂ – LiNbO₃", (Doctoral dissertation). Disponible at <<http://hdl.handle.net/11449/102528>>.
- [27] R.C. Lucacel, C. Marcus, I. Ardelean, FTIR and Raman spectroscopic studies of copper doped 2GeO₂-PbO-Ag₂O glasses, *J. Optoelectron. Adv. M.* 9 (3) (2007) 747.
- [28] N. Parveen, V.M. Jali, S.T. Patil, Structure and optical properties of TeO₂ – GeO₂ glasses, *Int. J. Adv. Sci. Eng. Technol.* 3 (2016).
- [29] T.T. Fernandez, et al., Role of ion migrations in ultrafast laser written tellurite glass waveguides, *Opt. Express* 22 (2014) 15298–15304.